Bažant, Z.P. (1984). "Numerical simulation of rogressive fracture in concrete structures: recent developments," Preprints, *Int. Conf. on Computer-Aided Analysis and Design of Concrete Structures*, held in Split,Yugoslavia, ed. by E. Hinton, R. Owen and F. Damjanic, University of Wales, Swansea, U.K., 1–17.

Proceedings of the International Conference on

Computer-Aided Analysis and Design of Concrete Structures

Part I

Edited by:

F. Damjanić
University of Split, Yugoslavia.

E. Hinton
University College, Swansea, U.K.

D. R. J. Owen
University College, Swansea, U.K.

N. Bićanić
University of Zagreb, Yugoslavia

V. Simović
Institute of Civil Engineering, Zagreb, Yugoslavia

Proceedings of the International Conference held at Split, Yugoslavia, 17th-21st September, 1984

PINERIDGE PRESS

Swansea, U.K.

NUMERICAL SIMULATION OF PROGRESSIVE FRACTURE IN CONCRETE STRUCTURES: RECENT DEVELOPMENTS

Zdeněk P. Bažant
Professor of Civil Engineering and Director,
Center for Concrete and Geomaterials
The Technological Institute
Northwestern University
Evanston, Illinois, 60201, U.S.A.

Abstract

The lecture deals with failure analysis of structures which exhibit distributed cracking. First, a continuum model which permits distributed cracking to occur over finite zones of the material is presented, and then the method of finite element analysis is described. The problem of formulating strain-softening relations under general loading histories is also discussed, and numerical examples are presented.

Introduction

Structures made of a heterogeneous brittle material such as concrete often exhibit brittle failures in which the material progressively fractures and the fracturing is distributed over a zone of finite size. In the continuum approximation, the behavior of such a fracturing zone is characterized by strain-softening, that is, a stress-strain relation in which the maximum principal stress decreases at increasing strain. Strain-softening may be easily implemented in a finite element code, however, problems are encountered in convergence as the mesh is refined. Using a finite element discretization of the classical, local continuum, the failure zone always localizes into a zone of vanishing thickness, which means that in the limit of an infinitely small mesh size the structure is indicated to dissipate negligible energy during failure. This aspect is obviously incorrect, and it causes an unacceptable sensitivity of the results to the chosen element size [1-5].

An expedient remedy is possible with the crack band model, in which the cracking front is forced to have a fixed width which is a material property. This type of analysis has been shown to yield good agreement with all important fracture test data for concrete, as well as rock [5,4]. However, a disconcerting feature remains from the theoretical point of view.

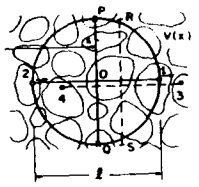

Fig. 1 - Representative Volume of an Aggregate Material.

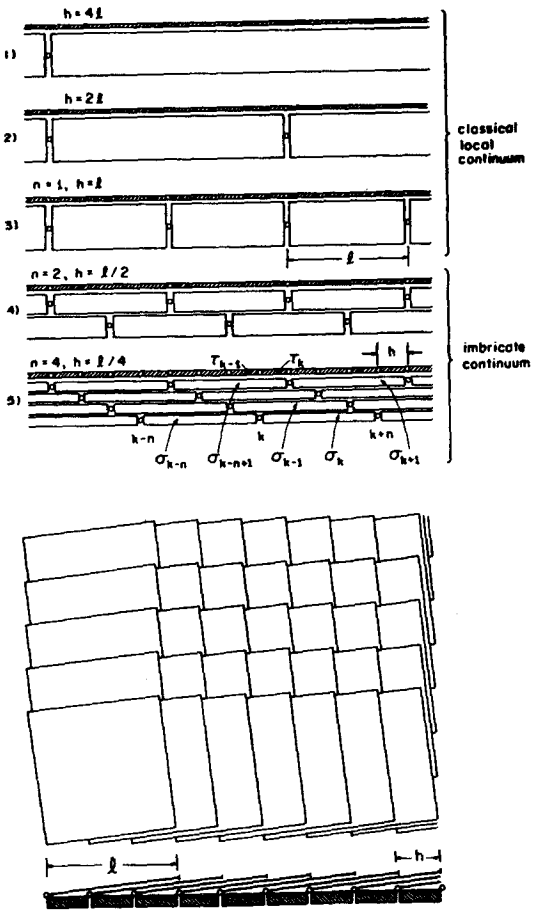

Fig. 2 - Finite Element Discretization of Imbricate Nonlocal Continuum for One Dimension and Two Dimensions (the continuum is the limiting case as the element size tending to zero).

One is not allowed to refine the mesh to sizes smaller than a certain characteristic length, and so one does not have a limiting continuum which the finite element model is supposed to approximate. To obtain such a model, it is necessary to abandon the idea of a classical, local continuum, as will now be shown in the first part of the lecture.

Nonlocal Continuum Model

From the works of Kröner and others [6-16], it is known that in a statistically heterogeneous medium which is not in a macroscopically homogeneous state of strain, the averaged (smoothed) stress at a certain point depends not only on the gradient of the averaged displacements at that same point (local properties), but also on the averaged displacements within a certain characteristic finite neighborhood of that point. The properties of such a medium cannot, therefore, be said to be local, and the medium is, therefore, called nonlocal.

The nonlocal displacement gradient may be defined by the relation

$$D_i u_j(\underset{\sim}{x}) = \frac{1}{V}\int_{V(\underset{\sim}{x})} \frac{\partial u_j(\underset{\sim}{x}')}{\partial x_i}\, dV' = \frac{1}{V}\int_{S(\underset{\sim}{x})} u_j(\underset{\sim}{x}')\, n_i(\underset{\sim}{x}')\, dS' \qquad (1)$$

in which u_j are the cartesian displacement components ($j = 1, 2, 3$), $\underset{\sim}{x}$ is the coordinate vector of the given point characterized by cartesian coordinates x_i, $V(\underset{\sim}{x})$ is the characteristic volume* of the material centered at point $\underset{\sim}{x}$, $S(\underset{\sim}{x})$ is the surface of this volume, $n_i(\underset{\sim}{x}')$ is the unit normal of this surface at point $\underset{\sim}{x}'$, and D_i is the gradient averaging operator. The surface integral in Eq. 1 follows from the volume integral by application of the Gauss integral theorem. More generally, a weighting function can be introduced in Eq. 1. Using the gradient averaging operator, the mean strains may be defined as

$$\bar{\varepsilon}_{ij} = \frac{1}{2}(D_i u_j + D_j u_i) \qquad (2)$$

In previous works dealing with nonlocal continua it has been generally assumed that the continuum equation of motion has the form

$$\frac{\partial}{\partial x_j}\, \bar{C}_{ijkm}(\bar{\underset{\sim}{\varepsilon}})\, D_m u_k = \rho \ddot{u}_i \qquad (3)$$

in which C_{ijkm} are secant elastic moduli which, in general, depend on the mean strain, ρ is the mass density, and superior dots refer to time derivatives. It is found, however, that Eq. 3 is incapable of describing a strain-softening continuum. It always leads to unstable response as soon as strain-softening begins. The difficulty has been traced to the asymmetry of these equations due to the combination of partial derivatives $\partial/\partial x_j$ with the gradient averaging operator D_m. This

*Fig. 1

feature gives rise to nonsymmetric finite element matrices even if C_{ijkm} are constant, i.e., if the medium is elastic. Such a nonsymmetry is certainly an unacceptable characteristic.

For this reason, a systematic derivation of the continuum equation of motion on the basis of Eq. 1 has been attempted, using the calculus of variations. It has been found [13-14] that the proper form of the continuum equation of motion is

$$(1-c)D_j \bar{C}_{ijkm}(\bar{\underset{\sim}{\varepsilon}})D_m u_k + c\,\frac{\partial}{\partial x_j} C_{ijkm}(\underset{\sim}{\varepsilon})\,\frac{\partial}{\partial x_m} u_k = \rho \ddot{u}_i \qquad (4)$$

in which c is an empirical coefficient between 0 and 1, and C_{ijkm} are the local secant moduli. In contrast to Eq. 3, each term of the last equation has a symmetric structure, and consequently, discretization by finite elements leads to symmetric stiffness matrices if the elastic moduli $\bar{C}_{ijkm}$ and C_{ijkm} are symmetric.

Eq. 4 can be also written in the form

$$(1-c)D_j \sigma_{ij} + c\,\tau_{ij,j} = \rho\,\ddot{u}_i \qquad (5)$$

in which

$$\sigma_{ij} = \bar{C}_{ijkm}(\bar{\underset{\sim}{\varepsilon}})\,\varepsilon_{km} = \bar{C}_{ijkm}(\bar{\underset{\sim}{\varepsilon}})D_m u_k \qquad (6)$$

$$\tau_{ij} = C_{ijkm}\,\varepsilon_{km} = C_{ijkm}\,\frac{\partial u_k}{\partial x_m} \qquad (7)$$

in which τ_{ij} are the usual, local stresses, and σ_{ij} are the stresses characterizing the stress state in the entire representative volume of the material and are called the broad-range stresses [13,14].

When the continuum defined by Eq. 4 is discretized by finite elements the size of which is smaller than the size ℓ of the representative volume, one obtains a system of overlapping (or imbricated) finite elements visualized in Fig. 2. Therefore, the present type of nonlocal continuum has been called imbricate. The finite elements keep a constant size ℓ as the mesh is refined, and the number of finite elements crossing a given point is inversely proportional to the mesh size, while the cross section of these elements diminishes so that all imbricated elements have the same total cross section for any mesh size. It can be also shown that the limiting case of the finite difference equations describing such an imbricated system of finite elements is the differential equation in Eq. 4 [13,14]. If the finite element size h is larger than the characteristic length ℓ, then the finite element model of the imbricate continuum becomes identical to that for the classical local continuum.

To assure convergence and stability, the local stress-strain relations (Eq. 7) may not exhibit strain-softening, or else unstable response and spurious sensitivity to mesh size, along with incorrect convergence, may be obtained. The strain-softening properties must be described solely by the broad-range stress-strain relation in Eq. 6.

Fig. 3 reproduces some of the results of explicit dynamic finite element calculations from Ref. 13, in which wave propagation in a strain-softening bar of length ℓ was analyzed. Both ends of the bar are subjected to a constant outward velocity d beginning at time t = 0. This loading produces step waves of strain propagating inward. When these waves meet at midlength, the strain suddenly increases and strain-softening ensues. If this problem is analyzed with the usual finite element method for local continuum, it is found that strain-softening is always limited to a single-element width. Thus, the width of the strain-softening zone reduces to zero as the element mesh is refined.* As a consequence, the energy W consumed by failure decreases with decreasing mesh size and approaches zero as the mesh size tends to zero (Fig. 5). Moreover, the finite element model of local continuum exhibits a discontinuous dependence of response on the prescribed end velocities as well as on the slope E_t of the strain-softening branch. The solution, however, converges to a unique exact solution, although this solution is unrealistic from the physical point of view.

By contrast, for the present imbricate continuum, the solution of wave propagation in the strain-softening bar (Fig. 3) exhibits correct convergence with a strain-softening zone of a finite size in the limit. Also, the energy consumed by failure in the bar converges to a finite value, as shown in Fig. 5. The characteristic length in these computations has been considered as $\ell = L/5$.

Differential Equations for Imbricate Continuum

For the purpose of analytical solutions it may be useful to approximate the integral operator that defines the mean strain by a differential operator. To this end, we expand the integrand of Eq. 1 into Taylor series;

$$u_{j,i}(\underset{\sim}{x}') = u_{j,i}(\underset{\sim}{x}) + u_{j,ik}(\underset{\sim}{x})\,x'_k + \tfrac{1}{2}\,u_{j,ikm}(\underset{\sim}{x})\,x'_k\,x'_m + \ldots$$

This yields

$$D_i u_j(\underset{\sim}{x}) = u_{j,i}(\underset{\sim}{x}) + \frac{1}{2!}\,A_{km}\,u_{j,ikm}(\underset{\sim}{x}) + \frac{1}{4!}\,B_{kmpq}\,u_{j,ikmpq}(\underset{\sim}{x}) + \ldots \qquad (8)$$

where $A_{km} = \frac{1}{V}\int_V x_h\,x_m\,dV = \frac{\ell^2}{20}\,\delta_{km}$ (9)

*Fig. 4

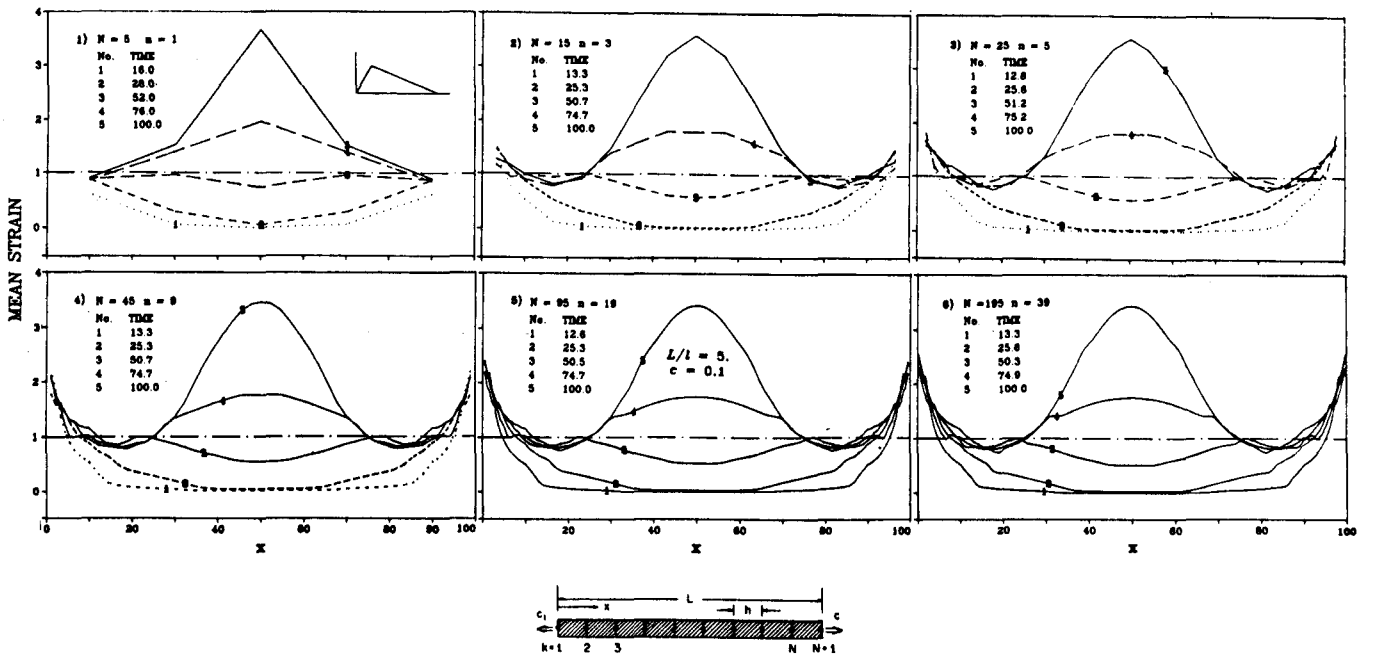

Fig. 3 - Numerical Results for Strain Distributions at Various Times for Wave Propagation in a Strain-Softening Bar, obtained for Subdivions with 5 to 195 Elements (characteristic length of material = L/5; element arrangement shown in Fig. 3) (after Bažant, Chang and Belytschko, 1983).

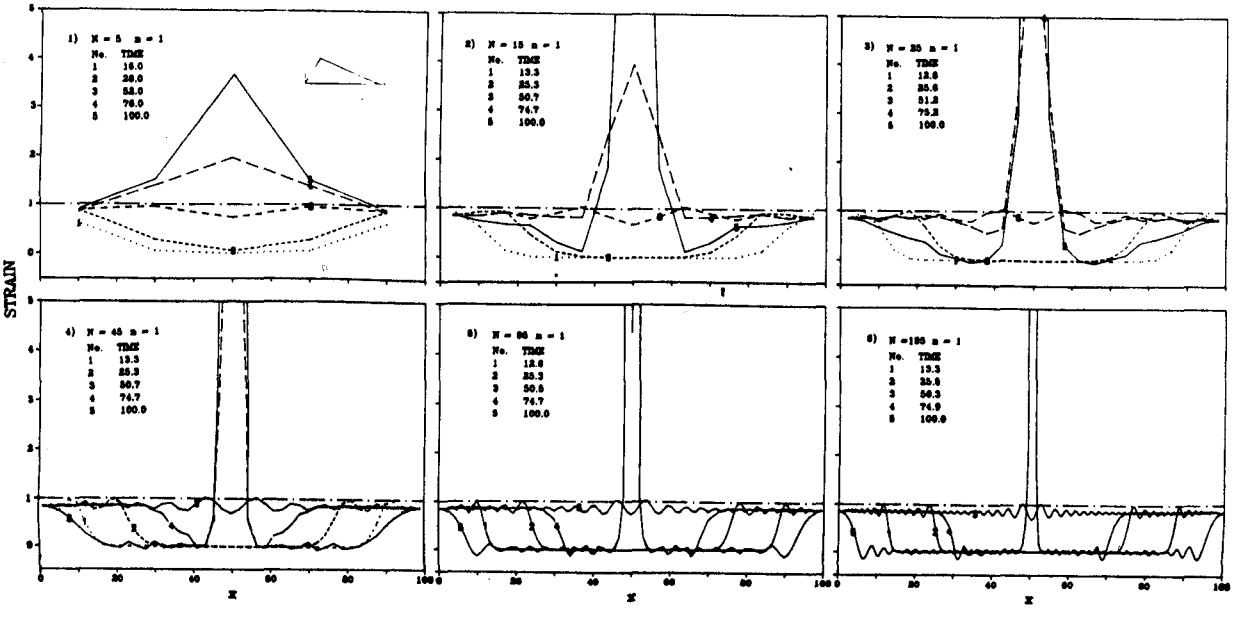

Fig. 4 - Numerical Results for the Same Problem as in Fig. 3 Obtained with Finite Elements of Classical Local Continuum.

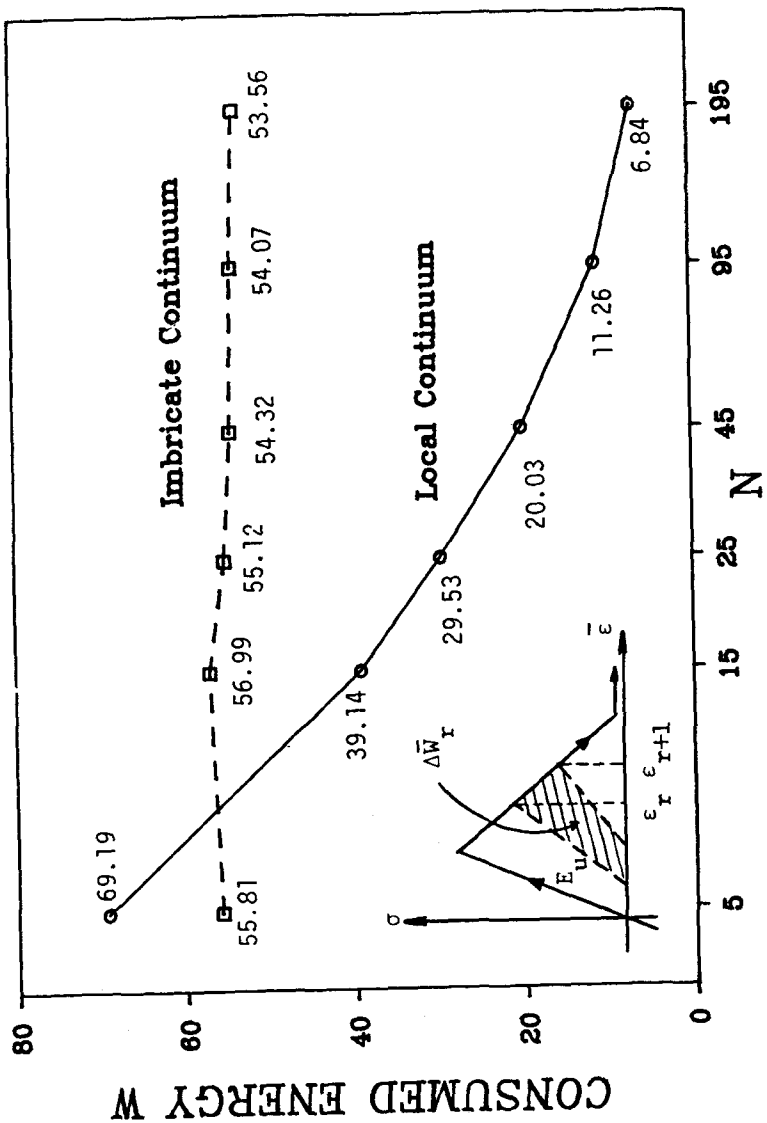

Fig. 5 - Numerical Results for Energy Consumed by Failure as a Function of Mesh Size, (a) for Classical Local Continuum, (b) for Imbricate Nonlocal Continuum (wave propagation in a bar, element arrangement shown in Fig. 3) (after Bažant, Chang, and Belytschko, 1983).

$$B_{kmpq} = \frac{1}{V} \int_V x_k\, x_m\, x_p\, x_q\, dV \tag{10}$$

if the representative volume is considered as a sphere of diameter ℓ. Neglecting terms of higher than second degree, we obtain

$$D_i\, u_j = u_{j,i} + \lambda^2\, u_{j,ikk} = (1 + \lambda^2 \nabla^2)\, \frac{\partial u_j}{\partial x_i} \tag{11}$$

in which $\lambda = \ell^2/40$ and ∇^2 = Laplace operator. Since ℓ equals approximately $3d_a$ where d_a = maximum aggregate size, we note that λ approximately equals the maximum aggregate radius. In view of Eq. 11, the field equations for the imbricate nonlocal continuum (Eqs. 5-6) at c=0 may now be written as follows

$$(1 + \lambda^2\, \nabla^2)\, \sigma_{ij,j} = \rho\, \ddot{u}_i \tag{12}$$

$$\sigma_{ij} = C_{ijkm}(\underset{\sim}{\varepsilon})\, \bar{\varepsilon}_{km} \tag{13}$$

$$\bar{\varepsilon}_{km} = (1 + \lambda^2\, \nabla^2)\, \varepsilon_{km} \tag{14}$$

$$\varepsilon_{km} = \frac{1}{2}\, (u_{k,m} + u_{m,k}) \tag{15}$$

Here we omitted the local terms, i.e., we set c=0. As we will see, the differential form is stable even if c=0.

The principle of virtual work for a body (whose domain is B and surface is S) made of the imbricate continuum may be stated as follows;

$$\delta W = \int_B \sigma_{ij}\ \delta\bar{\varepsilon}_{ij}\, dV - \int_S p_i\, \delta u_i\, dS + \int_B \rho\ddot{u}_i\, \delta u_i\, dV = 0 \tag{16}$$

in which $\delta u_i(\underset{\sim}{x})$ is any kinematically admissible displacement variation, and p_i and t_i are the given distributed surface and volume loads. Substituting Eq. 14 for $\bar{\varepsilon}_{ij}$ and applying repeatedly Gauss integral theorem, one can derive the field equations (Eqs. 12-15) from the virtual work relation (Eq.16). Moveover, the variational procedure yields the boundary conditions at surface S;

$$\text{either } u_i = 0 \text{ or } \bar{\sigma}_{ij}\, n_j = p_i \qquad (\text{on S}) \tag{17}$$

where

$$\bar{\sigma}_{ij} = (1 + \lambda^2\, \nabla^2)\, \sigma_{ij} \tag{18}$$

In the classical nonlocal continuum theory, the mean

strain is more generally defined with the help of a certain given weighting function $w(\underset{\sim}{r})$ where $\underset{\sim}{r} = \underset{\sim}{x}' - \underset{\sim}{x}$, i.e.,

$$V D_i u_j(\underset{\sim}{x}) = \int_{V(\underset{\sim}{x})} w(\underset{\sim}{r}) \frac{\partial u_i(\underset{\sim}{x}')}{\partial \underset{\sim}{x}_j'} dV' \tag{19}$$

in which $\int_V w(\underset{\sim}{r})\, dV' = 1$ (normalized weights). Introducing again the Taylor series expansion of $\partial u_i/\partial x_j'$ and truncating it after the quadratic term, one finds that

$$\bar{\varepsilon}_{ij}(\underset{\sim}{x}) = (1 + \alpha \lambda^2 \nabla^2)\, \varepsilon_{ij} \tag{20}$$

in which

$$\alpha = \frac{1}{2} \int_V w(\underset{\sim}{r})\, x_k'\, x_k'\, dV' \tag{21}$$

However, as long as λ is to be calibrated empirically, one can determine only the product $\alpha \lambda^2$, and not α and λ^2 separately. Thus, it does not matter which weighting function is used, and the simplest case $w(\underset{\sim}{r}) = 1/V = \text{const.}$ may be chosen.

It is interesting to compare the equation

$$\bar{\varepsilon}_{ij} = \varepsilon_{ij} + \frac{1}{2} \lambda^2 (u_{i,jkk} + u_{j,ikk})$$

with the well-known couple stress theories or micropolar theories. In them, only first and second derivatives of displacements appear, while here only first and third derivatives appear and the second derivatives are skipped. Moreover, there is no need to associate with the higher displacement derivative any special type of stress tensor of a higher rank, such as the couple stress tensor. Only one, second-rank stress tensor is used here.

Let us now check stability of the continuum. Consider linearly elastic properties, characterized by Young's modulus E, and the one-dimensional case, with $x_1 = x$, $u_1 = u$. From Eqs. 12-15 we obtain the differential equation of motion

$$\left(1 + \lambda^2 \frac{\partial^2}{\partial x^2}\right)^2 \frac{\partial^2 u}{\partial x^2} = \frac{\rho}{E} \frac{\partial^2 u}{\partial t^2} \tag{22}$$

Now seek a solution of the form $u = A \exp[i\, \omega(x - vt)]$ where v = wave velocity, ω = frequency. Substitution in Eq. 22 provides the condition

$$v^2 = \frac{E}{\rho} (1 - \lambda^2 \omega^2)^2 \tag{23}$$

We see that the wave velocity is always real. Thus, the approximation by derivatives of the imbricate continuum is stable even without the local terms in Eqs. 4 and 5, i.e. for c=0.

The chief advantage of the approximation by derivatives is that it facilitates analytical solutions, for which the boundary layer method known from fluid mechanics may be utilized. For computer programing, the use of imbricated finite elements (Fig. 1) seems, however, the simplest approach, since ordinary finite elements may be used and the nonlocal properties are entirely taken care of by the element imbrication (overlapping). Existing finite element codes and the usual element types can be used and one only needs to properly define the integer matrix giving the nodal numbers corresponding to each element number.

Crack Band Theory for Progressive Fracturing

For very fine meshes for which the element size h is less than the characteristic length ℓ of the medium, the fracture front may be many elements in width. However, for most practical applications it is sufficient to use finite elements whose size is equal to the characteristic length or is larger. In such a case, the cracking zone is of single element width at its front, and the finite element model of the imbricate continuum then coincides with that of the classical local continuum. The fracture analysis then becomes identical to what has been previously developed as the crack band theory [4,5].

Distributed cracking has been modeled in finite element analysis by adjustments in material stiffnesses since 1967 [16] when Rashid introduced this approach. Recently it has been demonstrated this approach yields consistent results, independent of the mesh size, only if the stress-strain relation with strain-softening is associated with a certain fixed finite element size, ℓ. For concrete, this size appears to be roughly $\ell = 3d_a$ where d_a = the maximum size of the aggregate. This size of finite elements is too small for many practical purposes. In the crack band theory it has been proposed and verified that consistent results can be obtained with larger finite elements provided that the tensile strain-softening relation is adjusted so that it yields the same fracture energy regardless of the mesh size. The fracture energy is expressed as

$$G_f = w_c \int \sigma_{33}\, d\varepsilon_{33} = \frac{w_c}{2} f_t'^2 \left(\frac{1}{E_0} - \frac{1}{E_t}\right) \tag{24}$$

in which ℓ now represents the width of the cracking front, σ_{33} and ε_{33} are the stress and strain in the finite element normal to the direction of cracking, f_t' is the direct tensile strength of the material, E_0 is the initial elastic Young's modulus, and E_t is the mean downward slope of the strain-softening segment of the stress-strain diagram, which is negative. If the finite element size is $h \pm \ell$, then Eq. 8 with ℓ replaced by h must

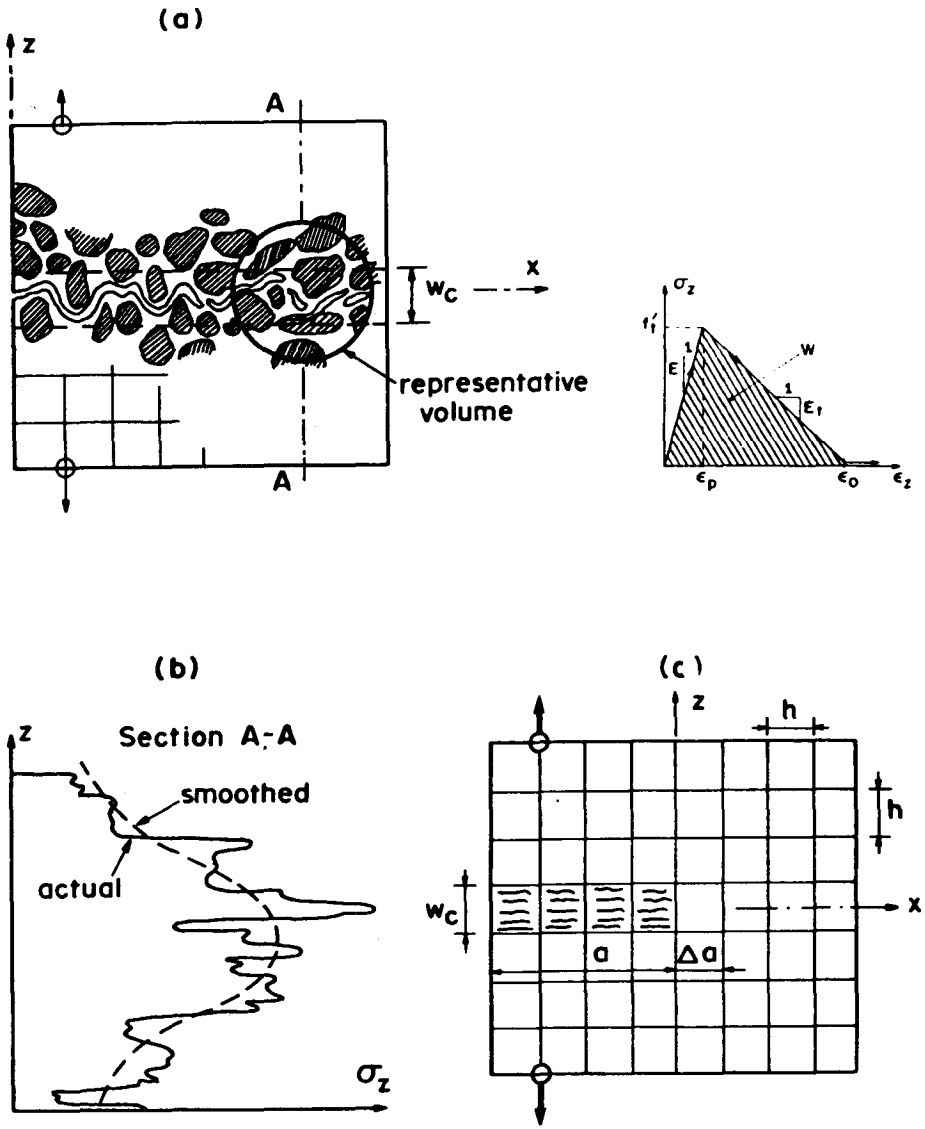

Fig. 6 - Crack Band Model and Corresponding Tensile Stress-Strain Relation with Strain-Softening.

yield the same value of G_f. This may be achieved by adjusting, first, the downward strain-softening slope E_t, and second, if the slope becomes vertical, by reducing the actual tensile strength f_t' to a certain equivalent strength f_{eq}' [1-5]. This type of model has been shown to agree with essentially all fracture test data for concrete, including the maximum load data and the R-curve data [4,5].

It may be noted that approximately the same results may also be obtained if the cracking strain accumulated across the width of the crack band is expressed as a single cracking displacement, and a certain stress-displacement relation in the connections between the finite elements is introduced into the analysis. This was the approach followed by Hillerborg et. al. [13].

Constitutive Relations for Strain-Softening

In the analysis of many practical situations, including all fracture tests, the principal stress direction in the fracture process zone remains constant during fracturing. Triaxial strain-softening can then be introduced in the form

$$\underset{\sim}{\varepsilon} = \underset{\sim}{D}\,\underset{\sim}{\sigma} + \underset{\sim}{\xi} \qquad (25)$$

Here $\underset{\sim}{\varepsilon}$ and $\underset{\sim}{\sigma}$ are the column matrices of the components of strain and stress, $\underset{\sim}{D}$ is the 6 x 6 matrix of elastic constants, and $\underset{\sim}{\xi}$ is a column matrix representing additional smeared-out strains due to cracking, $\underset{\sim}{\xi} = (\xi_{11}, \xi_{22}, \xi_{33}, 0, 0, 0)^T$. The normal stresses may be assumed to be uniquely related to their associated cracking strains,

$$\sigma_{11} = C(\xi_{11})\,\xi_{11}, \quad \sigma_{22} = C(\xi_{22})\,\xi_{22}, \quad \sigma_{33} = C(\xi_{33})\,\xi_{33} \qquad (26)$$

in which C is the secant modulus which reduces to zero at very large cracking strains and may be calibrated from direct tensile test data which cover strain-softening [17-24]. Different algebraic relations must, of course, be used for unloading.

For some situations, especially in dynamics, it is necessary to describe progressive formation of fracture during which the principal stress directions rotate. In such a case, the foregoing model is inadequate. A satisfactory formulation can be obtained with an analog of the slip theory of plasticity, which was called the microplane model [25,23]. In this model it is assumed that the strain on a plane of any inclination within the macroscopic smoothing continuum consists of the resolved components of one and the same macroscopic strain tensor ϵ_{ij}. Using the condition of equal energy dissipation when calculated in terms of the stresses and strains on all

such planes and in terms of the macroscopic stress and strain tensors, one may obtain the stress-strain relation

$$d\sigma_{ij} = D^c_{ijkm}\, d\,\varepsilon_{ij} \tag{27}$$

in which

$$D^c_{ijkm} = \int_0^{2\pi}\int_0^{\pi/2} n_i n_j n_k n_m\, F'(e_n)\, \sin\phi\, d\theta d\phi \tag{28}$$

This equation superimposes contributions to inelastic stress relaxations from planes of all directions within the material, defined by spherical coordinates θ and ϕ; n_i are the direction cosines for all such directions, and $F(e_n)$ is a function characterizing the constitutive properties and representing the stress-strain relation for one particular microplane within the material; $e_n = n_i\, n_j\, \varepsilon_{ij}$ = normal strain on a plane with direction cosines n_i. It has been demonstrated that the microplane model allows describing tensile strain-softening under general stress or strain histories and always leads to a reduction of stress to zero at sufficiently large tensile strain.

Conclusion

The concept of imbricate nonlocal continuum, along with strain-softening stress-strain relations, allows a mathematically consistent and realistic description of progressive distributed cracking in concrete structures.

Acknowledgment. - Partial financial support under AFOSR Grant No. 83-0009 to Northwestern University is gratefully acknowledged. Mary Hill is thanked for her exemplary secretarial assistance.

References

1. Bažant, Z. P., and Cedolin, L.,
"Blunt Crack Band Propagation in Finite Element Analysis,"
Journal of the Engineering Mechanics Division, ASCE,
Vol. 105, No. EM2, April 1979, pp. 297-315.

2. Bažant, Z. P., and Cedolin, L.,
"Fracture Mechanics of Reinforced Concrete,"
Journal of the Engineering Mechanics Division, ASCE,
Vol. 106, No. EM6, Proc. Paper 15917, December 1980,
pp. 1287-1306; with Discussion and Closure in Vol. 108,
1982, EM., pp. 364-471.

3. Bažant, Z. P., and Cedolin, L.,
"Finite Element Modeling of Crack Band Propagation,"
Journal of Structural Engineering, ASCE, Vol. 109, No. ST2
Feb. 1983, pp. 69-92.

4. Bažant, Z. P.,
"Crack Band Model for Fracture of Geomaterials,"
Proc., 4th Intern. Conf. on Numerical Methods in Geomechanics, held in Edmonton, Alberta, Canada, June 1982,
ed. by Z. Eisenstein, Vol. 3.

5. Bažant, Z. P., and Oh, B. H.
"Crack Band Theory for Fracture of Concrete,"
Materials and Structures (RILEM,Paris), Vol. 16, 1983
pp. 155-177.

6. Kröner, E.,
"Elasticity Theory of Materials with Long-Range Cohesive Forces,"
International Journal of Solids Structures, Vol. 3, 1967,
pp. 731-742.

7. Kröner, E.,
"Interrelations Between Various Branches of Continuum Mechanics,"
Mechanics of Generalized Continua, ed by E. Kröner,
Springer-Verlag, 1968, pp. 330-340.

8. Krumhansl, J. A.,
"Some Considerations of the Relation Between Solid State Physics and Generalized Continuum Mechanics,"
Mechanics of Generalized Continua, ed. by E. Kröner,
Springer-Verlag, 1968, pp. 298-311.

9. Kunin, I. A.
"The Theory of Elastic Media With Microstructure and the Theory of Dislocations,"
Mechanics of Generalized Continua, ed. by E. Kröner,
Springer-Verlag, 1968, pp. 321-328.

10. Levin, V. M.
"The Relation Between Mathematical Expectation of Stre and Strain Tensors in Elastic Microheterogeneous Media, Prikladnaya Matematika i Mekhanika, Vol. 35, 1971, pp. 694-701 (in Russian).

11. Eringen, A. C., and Edelen, D. G. B.
"On Nonlocal Elasticity,"
International Journal of Engineering Science, Vol. 10, 1972, pp. 233-248.

12. Eringen, A. C., and Ari, N.
"Nonlocal Stress Field at Griffith Crack,"
Cryst. Latt. Def. and Amorph. Mat., Vol. 10, 1983, pp. 33-38.

13. Bažant, Z. P., Chang, T. P., and Belytschko, T. B.
"Continujm Theory for Strain Softening,"
Report No. 83-11/428c, Center for Concrete and Geomaterials, Northwestern University, Evanston, Illinois, Nov. 1983.

14. Bažant, Z. P.,
"Imbricate Continuum: Variational Formulation,"
Report No. 83-11/428i, Center for Concrete and Geo-Materials, Northwestern University, Evanston, Illinois, Nov. 1983.

15. Hillerborg, A., Modéer, M., and Petersson, P. E.
"Analysis of Crack Formation and Crack Growth in Concrete by Means of Fracture Mechanics and Finite Elements,"
Cement and Concrete Research, Vol. 6, 1967, pp. 773-782.

16. Rashid, Y. R.
"Analysis of Prestressed Concrete Pressure Vessels,"
Nuclear Engng. and Design, Vol. 7, No. 4, April 1968, pp. 334-344.

17. ASCE State-of-the-Art Report on
"Finite Element Analysis of Reinforced Concrete,"
Prepared by a Task Committee charied by. A. Nilson, Am. Soc. of Civil Engrs., New York, 1982.

18. Wittmann, F. H. (editor)
"Fracture Mechanics of Concrete"
Elsevier, Netherlands, 1983.

19. Petersson, P. E.
"Fracture Energy of Concrete: Method of Determination"
Cement and Concrete Research, Vol. 10, 1980, pp. 78-89

"Fracture Energy of Concrete: Practical Performance and Experimental Results"
Cement and Concrete Research, Vol. 10, 1980, pp. 91-101.

20. Petersson, P. C.
"Crack Growth and Development of Fracture Zones in Plain Concrete and Similar Materials"
Doctoral Dissertation, Lund Institute of Technology, Lund, Sweden, Dec. 1981.

21. Evans, R. H., and Marathe, M. S.
"Microcracking and Stress-Strain Curves for Concrete in Tension"
Materials and Structures (RILEM, Paris), No. 1, Jan-Feb. 1968, pp. 61-64.

22. Heilmann, H. G., Hilsdorf, H. H., and Finsterwalder, K.
"Festigkeit und Verformung von Beton unter Zugspanungen: Deutscher Ausschuss fur Stahlbeton, Heft 203, W. Ernst & Sohn, West Berlin, 1969.

23. Bažant, Z. P.
"Fracture in Concrete and Reinforced Concrete,"
Chapter 13 in Mechanics of Geomaterials: Rocks, Concrete Soils, John Wiley & Sons, London, in press. (Proc. of W. Prager Symposium held at Northwestern University in Sept. 1983).

24. Reinhardt, H. W., and Cornelissen, H. A. W.
"Post-Peak Cyclic Behavior of Concrete in Uniaxial Tensile and Alternating Tensile and Compressive Loading"
Cement and Concrete Research, Vol. 14, 1984, pp. 263-270.

25. Bažant, Z. P., and Oh, B. H.
"Microplane Model for Fracture Analysis of Concrete Structures"
Proc. Symp. on the "Interaction of Nonnuclear Munitions with Structures," U. S. Air Force Academy, Colorado Springs, May 1983, pp. 49-55.